Cell, Vol. 83, 641–653, November 17, 1995, Copyright © 1995 by Cell Press

Disruption of the Murine Homeobox Gene *Cdx1* Affects Axial Skeletal Identities by Altering the Mesodermal Expression Domains of *Hox* Genes

Vasanta Subramanian,*† Barbara I. Meyer,†‡ and Peter Gruss‡
‡Department of Molecular Cell Biology
Max Planck Institute for Biophysical Chemistry
D-37077 Göttingen
Federal Republic of Germany
*School of Biology and Biochemistry
University of Bath
Bath BA2 7AY
England

Summary

***Cdx1* is expressed along the embryonic axis from day 7.5 postcoitum until day 12, by which time the anterior limit of expression has regressed from the hindbrain level to the forelimb bud region. To assign a functional role for *Cdx1* in murine embryonic development, we have inactivated the gene via homologous recombination. Viable fertile homozygous mutant mice were obtained that show anterior homeotic transformations of vertebrae. These abnormalities were concomitant with *posterior shifts of Hox gene expression domains* in the somitic mesoderm. The presence of putative *Cdx1*-binding sites in *Hox* gene control regions as well as in vitro transactivation of *Hoxa-7* indicates a direct regulation.**

Introduction

During mammalian embryonic development, the anteroposterior axis is generated at gastrulation with the formation of the primitive streak (Bellairs, 1986). The establishment of anteroposterior positional values along the embryonic axis seems to be determined at the time of cell ingression, being most obvious for the derivatives of the paraxial mesoderm. The paraxial mesoderm becomes segmented in discrete somites, which give rise later in development to the body musculature, the skin, and the different vertebrae of the axial skeleton (Dawes, 1930). Transplantation studies performed in the chick embryo demonstrated that heterografted unsegmented mesoderm from an original thoracic region gives rise to rib-carrying vertebrae (Kieny et al., 1972), indicating that the still unsegmented mesoderm already shows anteroposterior specification.

The clustered *Hox* genes are believed to play a key role within this process (for review see McGinnis and Krumlauf, 1992). The *Hox* genes start expression early in the primitive streak and establish nonidentical overlapping expression domains along the axis later in development. The regional identity of the paraxial mesoderm seems to be conferred by the combined expression of the clustered *Hox* genes (for reviews see Hunt and Krumlauf, 1992; Mavilio, 1993). Experimental alteration of *Hox* gene expression in transgenic mice (Kessel et al., 1990) and by retinoic acid (RA) (Kessel and Gruss, 1991) results in homeotic transformations in the axial skeleton. The role of *Hox* genes in conferring regional identity to the paraxial mesoderm has been further confirmed by the phenotypes obtained by targeted mutation of several members of the *Hox* gene family, which leads to transformations of the axial skeleton (for review see Krumlauf, 1994).

On the basis of expression pattern and functional analysis, members of the *caudal*-type homeobox gene family also seem to play a role in the processes of axis organization, specification, or both. The first member to be isolated, the *caudal* gene in Drosophila (Mlodzik et al., 1985), is expressed in a gradient that peaks at the posterior pole of the embryo (Mlodzik and Gehring, 1987). Functional analysis demonstrated that in the *caudal* mutants there is a loss of posterior structures (Macdonald and Struhl, 1986), while the ectopic expression of *caudal* leads to a disruption of head segmentation and development (Mlodzik et al., 1990).

Several other *caudal*-like genes have been isolated in various species; these include *Cdx1* (Duprey et al., 1988), *Cdx2* (James and Kazenwadel, 1991), and *Cdx4* (Gamer and Wright, 1993) in mouse, *Cdx3* (German et al., 1992) in hamster, *CHox-cad* (Frumkin et al., 1991) and *CHox-cad2* (Serrano et al., 1993) in chicken, *Xcad1*, *Xcad2* (Blumberg et al., 1991), and *Xcad3* (Northrop and Kimelman, 1994) in Xenopus laevis, *zfcdx* (Joly et al., 1992) in zebrafish, *B mori caudal* (Xu et al., 1994) in silk moth, and *ceh-3* in Caenorhabditis elegans (Bürglin et al., 1989). All of these genes are expressed at gastrulation.

The developmental mutant *pal-1* in C. elegans, which shows anterior homeotic transformation, has been correlated with the *caudal*-type gene *ceh-3* (Waring and Kenyon, 1990, 1991). Genetic analysis indicates that *ceh-3* acts by misregulation of the clustered homeotic gene *mab-5* (Kenyon, 1986).

The murine *caudal*-like gene *Cdx1* is first expressed at 7.5 days postcoitum (dpc) in the primitive streak. Later in development, the expression extends posteriorly along the entire embryo to an anterior limit within the presumptive posterior hindbrain (Meyer and Gruss, 1993).

To assign a functional role for *Cdx1* in murine development, we have inactivated *Cdx1* by homologous recombination.

The disruption of *Cdx1* led to axial skeletal abnormalities with anterior homeotic transformation. These transformations were accompanied by a posterior shift in the expression of *Hox* genes in the somites. The presence of putative *Cdx1*-binding sites within the regulatory sequences of *Hox* genes and in vitro transactivation of *Hoxa-7* by *Cdx1* suggest a direct interaction, resulting in the establishment of correct *Hox* gene expression pattern in the somitic mesoderm.

†The first two authors have contributed equally to this work.

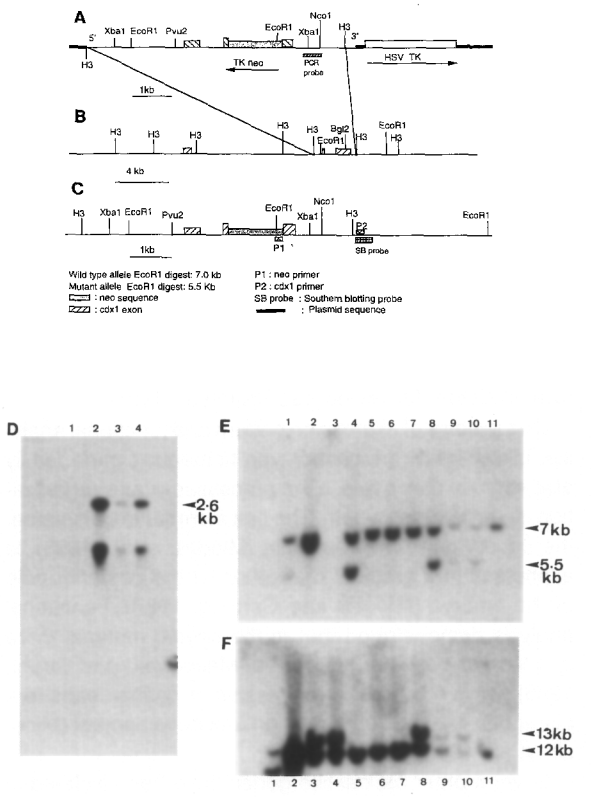

Figure 1. Genomic Organization, Targeting Vector, and Analysis of Recombinant Clones

(A) Diagram of the targeting vector.

(B) *Cdx1* genomic sequence.

(C) Organization of the disrupted allele. The arrowheads in (A) represent the transcriptional orientation of the *neo* and *tk* genes. The approximate positions of the PCR primers are indicated as P1 and P2.

(D) PCR analysis of the transfected ES cells. Lane 1 is a wild-type clone; lanes 2, 3, and 4 show the characteristic 2.6 kb band expected from the disrupted allele with primers P1 and P2 indicated in (C). An unexplained band of lower molecular mass also appears in all the clones that show a positive PCR signal for the targeted allele.

(E) Southern blot of wild-type and targeted ES cell DNA digested with EcoRI and probed with the SB probe indicated in (C). The wild-type band is 7.0 kb, and the mutant is 5.5 kb. Lanes 1, 4, 8, 9, and 10 are of DNA from recombinant clones, and 2, 5, 6, 7, and 11 are of DNA of wild-type clones.

(F) Southern blot analysis of wild-type and targeted ES cell DNA digested with BamHI and probed with the SB probe indicated in (C). The wild-type allele gives a 12 kb band, and the mutant allele shows a 13 kb band, owing to the presence of the 1.0 kb *neo* gene.

Results

Targeted Mutation of *Cdx1* and Generation of Mutant Mice

Mutant *Cdx1* mice were generated by homologous recombination using the positive/negative selection system (Mansour et al., 1988). The embryonic stem (ES) cell line RI (Nagy et al., 1993) was electroporated with the targeting construct (Figures 1A, 1B, and 1C). Southern blot analysis of 72 individual ES cell clones identified 14 correctly targeted clones, indicating a frequency of 1 in 5 (Figures 1E and 1F).

Five independent clones were injected into C57/BL6 blastocysts or aggregated with NMRI morulae, and from three male chimeras, obtained on each of these genetic backgrounds, germline transmission of the mutant *Cdx1* allele was obtained. The transmission of the *Cdx1* mutation was analyzed by Southern blotting of tail DNA from the progeny (Figures 2A and 2B). The heterozygous and homozygous progeny appeared to be normal in size and did not exhibit any overt signs of abnormality.

Cdx1$^{-/-}$ Mice Are Negative for the CDX1 Protein

The insertion of the neomycin (*neo*) gene in the opposite transcriptional orientation to *Cdx1* introduces a premature stop codon into the coding sequence, as indicated by the conceptual translation of the sequences of the fusion gene. The mutated gene should encode a truncated CDX1 protein, lacking the carboxy-terminal end that includes the recognition helix (Figure 2C). To determine whether a truncated CDX1 protein was present in the mutant homozygous mice, we carried out immunoblotting experiments using antibodies raised to the amino-terminal end of the CDX1 protein. The anti-CDX1 antibody recognizes a protein that has an apparent molecular mass of 36 kDa (Meyer and Gruss, 1993). In normal adult mice, the only detectable site of expression of *Cdx1* is the intestine (Duprey et al., 1988). Analysis of protein extracts from the intestines of 3-week-old adult *Cdx1*$^{-/-}$ and *Cdx1*$^{+/+}$ mice by immunoblots is shown in Figure 2D. In the *Cdx1*$^{-/-}$ mice, there was no detectable CDX1 protein in the various regions of the intestines, as compared with their wild-type littermates. It is most likely that the truncated protein, if synthesized, is not stable and is rapidly degraded (Capecchi et al., 1974; Rechsteiner, 1987).

Cdx1$^{-/-}$ Mice Exhibit Anomalies and Homeotic Transformations of Vertebrae

Skeletal preparations were made from *Cdx1*-deficient homozygotes as well as from their wild-type and heterozygous littermates. The heterozygous *Cdx1* mice were normal, and for further studies, comparisons were made only between the wild type and the homozygous *Cdx1* mutants. A total of 56 homozygous mice on an outbred NMRI, an inbred C57/BL6, and a 129/SV genetic background were analyzed, and the skeletal abnormalities are summarized in Table 1.

Abnormalities in the Cranial Regions

In all mutant mice, consistent abnormalities of the axial skeletal elements were observed, beginning with the occipital bones of the skull. The basioccipital bone was broader at its posterior end (Figures 3C and 3E; Figure 4), and in most of the mutants, incomplete neural arches were fused to it (Figure 4). In these mutants, the exoccipital bones were affected, as the occipital condyles are not well developed (Figure 4). Occasionally, the supraoccipital bone appeared broader (Figure 4).

Besides the aberrations in the basioccipital, exoccipital, and supraoccipital bones, there were no apparent pheno-

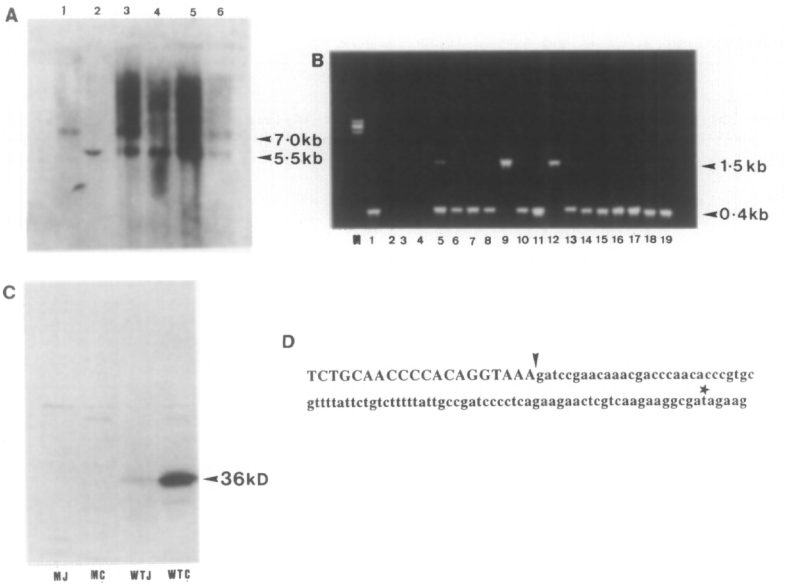

Figure 2. Southern Blot and PCR Analysis of the Genotypes of a Representative Litter Generated by a Heterozygous Cross, and Western Blot Analysis of Intestinal Extracts for the CDX1 Protein and the Predicted Fusion Protein Produced by the Insertion of the *neo* Gene

(A) Southern blot analysis of tail DNA from the offspring of a heterozygous mating. Tail DNA was digested with EcoRI and probed with the SB probe used to detect targeted cells and indicated in Figure 1C. DNA in lane 1 indicates a wild-type offspring, that in lanes 3 and 6 heterozygotes, and that in lanes 4 and 5 the mutant homozygotes.

(B) PCR analysis of DNA from extraembryonic membranes of 12.5 dpc embryos from a heterozygote intercross. The diagnostic wild-type PCR fragment amplified is 400 bp across the second intron, which increases to 1.5 kb after the insertion of the *neo* gene into the third exon.

(C) Western blot analysis of intestinal extracts for CDX1 expression. The 36 kDa band recognized by the anti-CDX1 antibody is indicated. MC, mutant colon; MJ, mutant jejunum; WTC, wild-type colon; WTJ, wild-type jejunum.

(D) The sequence of the fusion of the *Cdx1* exon with the *neo* gene. The uppercase letters represent the *Cdx1* coding sequence, and those in the lower case, the sequence of the *neo* gene. The arrow indicates the fusion site and the asterisk the stop codon introduced in the reading frame that deletes the third helix.

typic differences in the rest of the skull compartment between the wild type and the mutants (see Figure 3).

Vertebral Transformations

Typically, a wild-type mouse has seven cervical vertebrae (C1–C7), thirteen thoracic vertebrae (T1–T13), six lumbar vertebrae (L1–L6), three to four sacral vertebrae, and 31 caudal vertebrae. For the purposes of comparison, we have numbered the vertebrae consecutively, beginning with the first vertebra caudal to the basioccipital bone, even if this was only rudimentary or incomplete.

Vertebra 1

In a majority of the mutants, an incomplete vertebral neural arch was present, which was closely apposed to the basioccipital bone (see Table 1). Only the ventral aspects of this neural arch were developed. It was often fused to the basioccipital bone and hence did not show the anterior arch. This vertebral unit had a cotylar face and thick transverse processes, which are morphological characteristics of the first vertebra (atlas) (Figures 4 and 5). It was designated as vertebra 1 owing to its position and its characteristics. The normal atlas is unique in that it lacks a vertebral body, in place of which the dens of the axis is positioned. It has no true spinous process and has an anterior arch, the anterior arcus atlantis (AAA) (Figure 5B).

Vertebra 2

In 91% of the mutants analyzed, vertebra 2 had the following phenotype: a cotylar face, thick and laterally extending transverse processes, fusion dorsally with vertebra 3, and an underdevelopment of the AAA; some specimens also showed a detached vertebral body (odontoid element) (see Figures 3, 4, and 5). The wild-type vertebra 2 (axis) typically consists of two vertebral bodies. One, which is developmentally derived from the first vertebra, contributes to the odontoid process, the dens axis, which projects vertically from the vertebral body of the axis. When the atlas and the axis are articulated, the dens of the latter is retained against the anterior arch by the transverse ligament. This is the pivot on which the atlas moves. Only in a few mutant mice did vertebra 2 exhibit the characteristics of an axis (Figure 5A). On the whole, the morphology of vertebra 2 as an atlas-like structure in the mutants was determined by the degree with which vertebra 1 appeared as an occipital-like structure (see Figures 4 and 5).

Vertebra 3

The third vertebra in most of the mutant mice had axis characteristics (see Figure 3). Specifically, it had broad neural arches, occassionally split on the dorsal surface; the vertebral body was fused partially to the body of vertebra 2, indicating the development of a dens axis (see Figures 3C and 3E). In some mutant skeletons, the third vertebra had a mixed identity. It appeared with an axis morphology on one side and vertebra 3 morphology on the other side (Figure 5C). In the wild-type mice, vertebrae 3–5 appear similar. They have a foramen transversum and articular processes, which project within the plane of the body. The sixth vertebrae has in addition the diagnostic anterior tuberculi, while the articular processes project more laterally. The seventh vertebra lacks the foramen transversum (Figure 5B).

Vertebrae 4, 5, and 6

In the mutant *Cdx1*$^{-/-}$ mice, vertebrae 4 and 5 were indistinguishable from those in the wild type (Figure 5). However, vertebra 6 appeared with the morphological characteristics of vertebra 5. In 60% of the *Cdx1*$^{-/-}$ mice, vertebra 6 did not carry tuberculi anterior and developed articular proccesses, which project within the plane of the body (Figure 5A). In 21% of the cases, only one tuberculus anterior was present on vertebra 6, while the other side of the vertebra showed vertebra 5 morphology (Figure 5C).

Table 1. Skeletal Abnormalities in *Cdx1*$^{-/-}$ Mice

	Genetic Background			
	Cdx1$^{-/-}$			
Phenotypes	NMRI (n = 25) (%)	C57BL/6 (n = 17) (%)	129/SV (n = 14) (%)	*Cdx1*$^{+/+}$ (n = 25) (%)
Abnormalities of basioccipital	25 (100)	17 (100)	14 (100)	–
Abnormalities of vertebra 1	25 (100)	17 (100)	13 (92)	–
V1 malformed atlas (AAA incomplete or fused to V2)	1 (4)	–	5 (35)	–
V1 neural arches fused to basioccipital (no AAA, no lateral and dorsal bone structure)	24 (96)	17 (100)	8 (57)	–
Abnormalities of vertebra 2	25 (100)	17 (100)	14 (100)	–
V2 malformed axis (fused to AAA of V1 or broader dorsally)	–	–	5 (35)	–
V2 malformed atlas (dorsally broader, fused to dens axis)	25 (100)	17 (100)	9 (64)	–
Abnormalities of vertebra 3	25 (100)	17 (100)	8 (57)	–
V3 appears as malformed axis	23 (92)	13 (76)	7 (50)	–
Incomplete dens axis present				
Broad dorsally as in the normal axis but split	8 (32)	13 (76)	7 (50)	–
Fused dorsally to V2	6 (24)	5 (29)	–	–
Tuberculi anterior on				
V6 (bilateral)	2 (8)	4 (23)	3 (21)	25 (100)
V6 and V7 (unilateral)	1 (4)	8 (47)	3 (21)	–
V7 (bilateral)	21 (84)	5 (29)	8 (57)	–
Spinous process on				
V9	15 (60)	17 (100)	4 (28)	25 (100)
V10	7 (28)	–	4 (28)	–
V9 and V10	2 (8)	–	6 (42)	–
Absent	1 (4)	–	–	–
First ribs on				
V8 (bilateral)	24 (96)	17 (100)	13 (92)	25 (100)
V8 (unilateral)	1 (4)	–	–	–
V7	–	–	1 (7)	–
Number of true ribs				
7	22 (88)	17 (100)	9 (64)	25 (100)
8	3 (12)	–	5 (35)	–
Rib fusion				
R1 and R2 normal	8 (32)	15 (88)	5 (35)	25 (100)
R1 and R2 fused unilaterally	10 (40)	1 (4)	4 (28)	–
R1 and R2 fused bilaterally	7 (28)	1 (4)	5 (35)	–

Vertebra 7

In the mutant, this vertebra possessed a foramen transversum and tuberculi anterior uni- or bilaterally (Figures 5A and 5C), which are features of vertebra 6.

Thoracic Vertebrae

The 13 thoracic vertebrae have similar morphological features, except for vertebra 9, which has a prominent dorsal spinous process (Figure 5B). The first seven thoracic vertebrae bear the true ribs articulated to the sternum, while the following six vertebrae carry the false ribs. The head (capitulum) of the ribs actually articulates with the two centra of the thoracic vertebrae. The sternum consists of a series of discrete sternebrae.

In all the mutant mice, vertebra 8 bore the first pair of ribs, like the wild type, suggesting that it was the first thoracic vertebra. On the basis of the observed morphological changes of vertebra 7 to 6 and the presence of ribs on vertebra 8, there appears to be a loss of vertebra 7 identity in the mutant (Figure 5). However, in 80% of the mutants, vertebra 8 was characterized by an articular process with an upward thrust, a transverse process spaced ventral from the articular process and extending laterally, and a flat ellipsoid body with the rib neck and capitulum extending slightly ventrally. On the basis of these criteria, in some aspects vertebra 8 possesses some C7 characteristics, but has a pair of ribs reminiscent of T1.

The general morphology of vertebrae 9 to 20 of the mutants appeared as in the wild type. However, in 70% of the *Cdx1*-deficient mice, the prominent spinous process appears on vertebra 10 instead of vertebra 9. The first pair of ribs in the mutant mice are either unilaterally or bilaterally fused to each other before fusing with the sternum (Figures 6A–6E). The fusion of the following ribs to the sternum is shifted anteriorly by one sternebra, and in

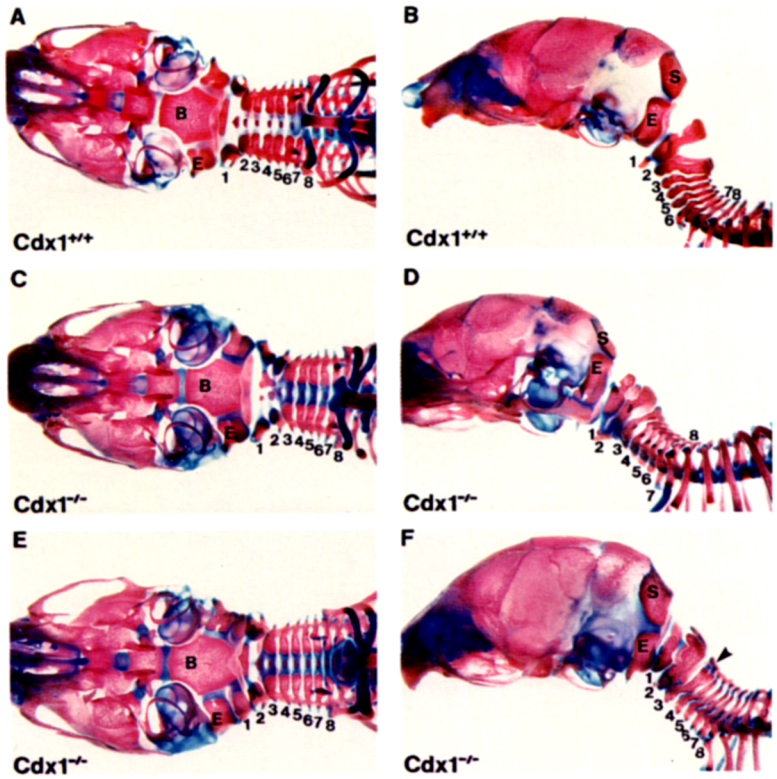

Figure 3. Skull Phenotypes in *Cdx1*$^{-/-}$ and Wild-Type Mice

The skeletons of newborn mice were stained with alcian blue and alizarin red and cleared in alkali and glycerol.

Ventral view (A) and lateral view (B) of a wild-type skull.

Ventral view (C and E) and lateral view (D and F) of a *Cdx1* mutant skull.

E, exoccipital bone; i, interparietal bone; s, supraoccipital bone; b, basioccipital bone.

20% of the animals, the total number of articulated ribs is increased to eight (Figures 6D and 6E), while the total number of ribs was maintained at thirteen. In some cases, where the fusion of the first pair of ribs to the second pair occurred, the number of sternebrae was reduced from five to four (Figure 6D).

Lumbar and Caudal Vertebrae

The number and morphology of all the lumbar and caudal vertebrae were apparently normal. The appendicular skeleton, of both the forelimbs and the hindlimbs, did not exhibit obvious abnormalities.

Thus, the disruption of *Cdx1* causes anterior homeotic transformation of vertebrae. The first vertebra developed into a more anterior structure, the basioccipital bone, and subsequent vertebrae up to the posterior thoracic ones assumed anterior identities.

Histological Examination of *Cdx1*$^{-/-}$ Mice

For a direct visualization of the effects of the *Cdx1* disruption on the patterning of the nervous system, the *Cdx1* mutant mice were crossed with the transgenic L17 *lacZ* line (Püschel et al., 1990, 1991). This transgenic line exhibits *lacZ* staining in most neuroectoderm-derived structures, such as the spinal and cranial ganglia and the associated nerves (Tremblay et al., 1995).

On the basis of the anterior transformation of the skeleton at the boundary between the skull and the cervical region, it could be possible that the neuroectoderm at this axial level is also affected. In wild-type embryos, the first spinal ganglion (Froriep's ganglion) degenerates by 12.5

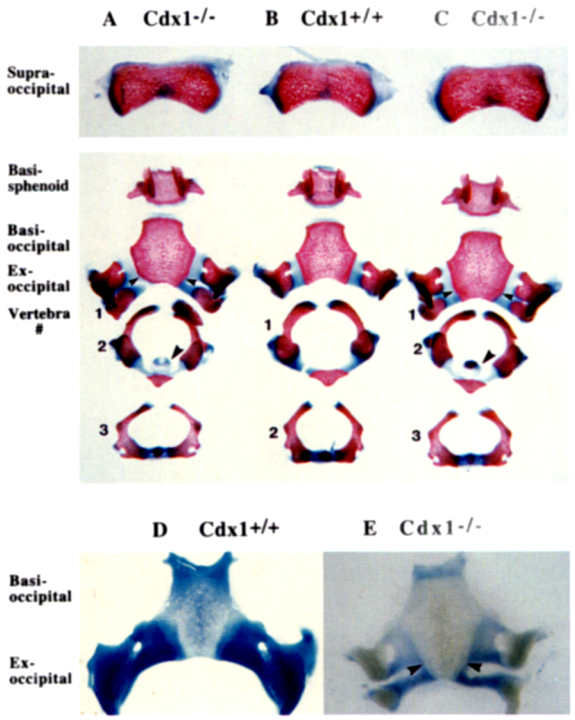

Figure 4. Transformations in the Basal Cranium and Cervical Region of *Cdx1*$^{-/-}$ Mice

Skeletal preparations from newborn wild-type (B) and mutant mice (A and C) and from 16.5 dpc wild-type (D) and mutant embryos (E). Arrows in the basioccipital bone indicate the area of broadening. Arrow in vertebra 2 shows the position of the detached centrum.

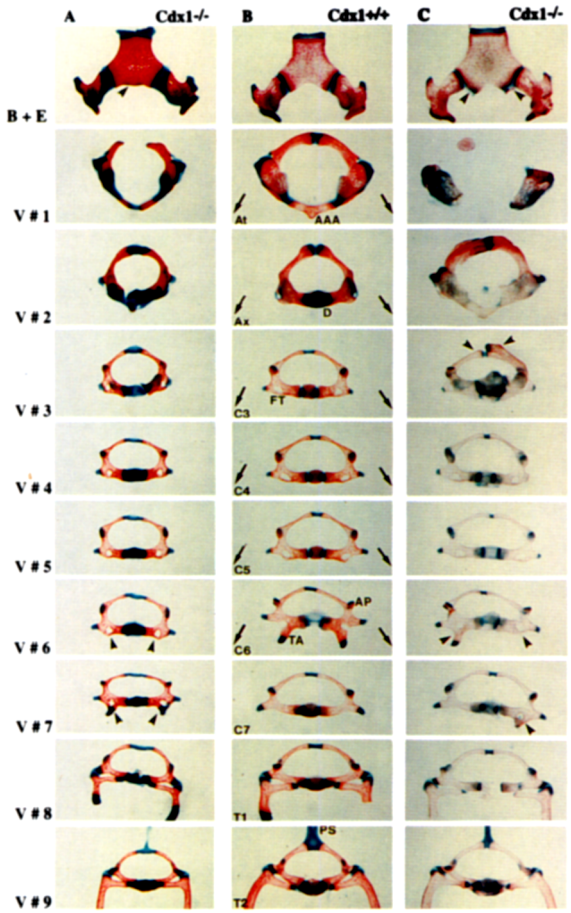

Figure 5. Morphology of Cervical and Thoracic Vertebrae

(A) and (C) represent mutant mice and (B) wild-type mice. Vertebrae are numbered consecutively from 1 to 9. Arrows in (B) indicate the identity of the corresponding vertebra of the mutant. Arrows in vertebra number 3, column (C), point to abnormal neural arches. Vertebra number 6 and vertebra 7 in column (C) show a single anterior tuberculus, indicated by arrows. Abbreviations are as follows: AAA, anterior arcus atlantis; AP, articular proccess; At, atlas; Ax, axis; C3–C7, cervical vertebrae; D, dens axis; T1–T2, thoracic vertebrae. B plus E indicates basioccipital and exoccipital bones; sp, spinous process. FT, foramen transversum; TA, tuberculi anterior; PS, process spinous.

dpc (Figures 7A–7C). An anterior transformation affecting the neuroectoderm of the axial level of prevertebra 2 should result in a degeneration of the second spinal ganglion. Histological analysis of 12.5 dpc *Cdx1*$^{-/-}$/L17 embryos showed no evidence for any consequences of the *Cdx1* mutation on the neuroectodermal tissues (Figure 7D). Even the first cranial nerve does not seem to be affected in its axial position between the condensation of the first prevertebra and the basioccipital bone, although a partial fusion of these structures occurred (Figure 7F).

However, other axial morphological landmarks, such as the vertebral artery, which normally bends dorsally anterior to prevertebra 1, have an altered position. In the mutant embryos, the axial level of the bending artery is shifted posteriorly between the first and the second prevertebrae (Figures 7E and 7F).

Hox Gene Expression in *Cdx1*$^{-/-}$ Mice

Functional analyses of several *Hox* genes have demonstrated their role in the specification of vertebral identities (for review see Krumlauf, 1994). The combination of *Hox* genes expressed by a given cell or group of cells seems to determine its or their future axial identity (Kessel and Gruss, 1991). To determine whether the axial skeletal abnormalities observed in the *Cdx1*$^{-/-}$ mice correlate with alterations of *Hox* gene expression boundaries, in situ hybridization was carried out. For anatomical landmarks to describe their anterior expression boundaries, we used the condensations of the basioccipital bone and the prevertebrae. The basioccipital bone is characterized by the cross of the hypoglossal nerve, leading to a V-shaped interruption of this condensation (Figures 8C, 8G, and 8K). The second morphological landmark is the visible double condensation of thoracic vertebrae, because of the additional condensation of the rib anlage. Therefore, the first double condensation marks the eighth prevertebra (Figures 8A, 8C, and 8O).

Since we observed aberrations in the base of the skull and clear anterior transformations along the axis, the expression of representative *Hox* genes belonging to different clusters, in particular *Hoxa-7*, *Hoxc-5*, *Hoxc-6*, *Hoxc-8*, and *Hoxd-3*, were investigated. Members of three *Hox* gene clusters that were analyzed showed a posterior shift in their expression domains in the prevertebrae (Figures 8 and 9; Table 2). For *Hoxc-6*, *Hoxc-8*, and *Hoxa-7*, the expression is shifted by one prevertebra; *Hoxc-5* showed a posterior shift by two prevertebrae. The expression pattern of *Hoxd-3*, examined at 9.5 dpc by whole-mount in situ hybridization, showed clearly a unchanged expression in the neuroectoderm at the boundary of rhombomeres 4 and 5 (Figures 9A and 9B). However, the mesodermal expression is shifted from somite 5 to somite 6 (as reference, we used the developing forelimb bud) (Figure 9C). Therefore, the mutation of *Cdx1* seems only to interfere with the establishment of the anterior expression boundaries of *Hox* genes in the somites, while their expression in the neuroectodermal lineages do not seem to be affected. These findings are in agreement with the restriction of the *Cdx1*$^{-/-}$ phenotype to the skeletal elements.

Transactivation of the *Hoxa-7* Promoter by *Cdx1*

Members of the caudal-type homeodomain proteins have been shown to function as transcription factors. The *caudal* gene in Drosophila acts as a direct activator of the segmentation gene *fushi tarazu* (*ftz*) (Dearolf et al., 1989). Furthermore, it has previously been shown that the hamster gene *Cdx3* activates the insulin gene (German et al., 1992), and mouse *Cdx2* is able to bind the SIF1 element and activates transcription of the sucrase-isomaltase promoter (Suh et al., 1995). Characterization of the binding sites of these genes within their target promoters allowed the identification of a conserved TTTATG motif. In addition, in vitro binding studies of the chicken *CdxA* on random oligonucleotides and genomic DNA fragments helped to define a consensus binding sequence of A/CTTTATA/G (Margalit et al., 1993). Taken together, these independent

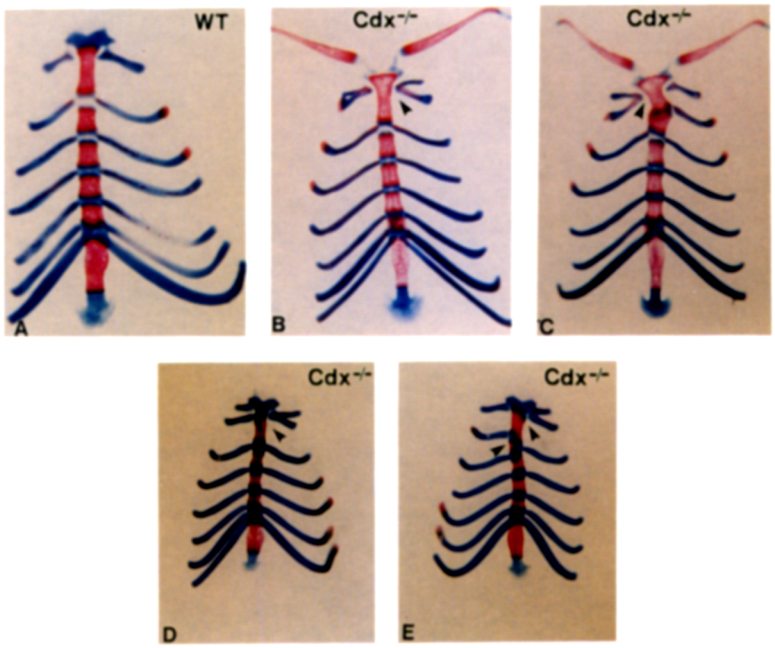

Figure 6. Morphological Features of the Sternum and Associated Ribs from Newborn Wild-Type and Mutant Mice Stained with Alizarin Red and Alcian Blue

Wild-type (A) and mutant (B, C, D, and E) sterna.

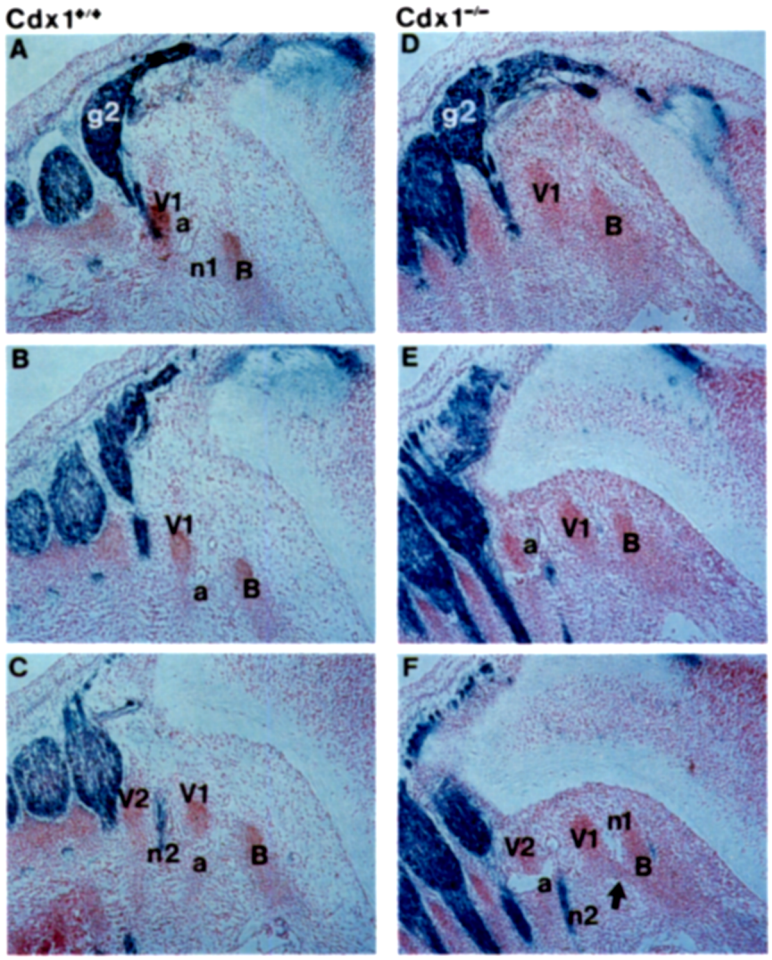

Figure 7. Histological Analysis of 12.5 dpc *Cdx1*$^{-/-}$/L17 and *Cdx*$^{+/+}$/L17 Embryos

Embryos were stained for *lacZ* activity, sectioned, and stained with neutral red.

(A), (B), and (C) are serial saggital sections of a wild-type/L17 embryo, and (D), (E), and (F) are sections of a *Cdx*$^{-/-}$/L17 embryo. Arrow indicates fusion of basioccipital with the first vertebra. Abbreviations: B, basioccipital bone; V1, prevertebra 1; n1, cranial nerve; n2, second spinal nerve; a, vertebral artery; g2, second spinal ganglion.

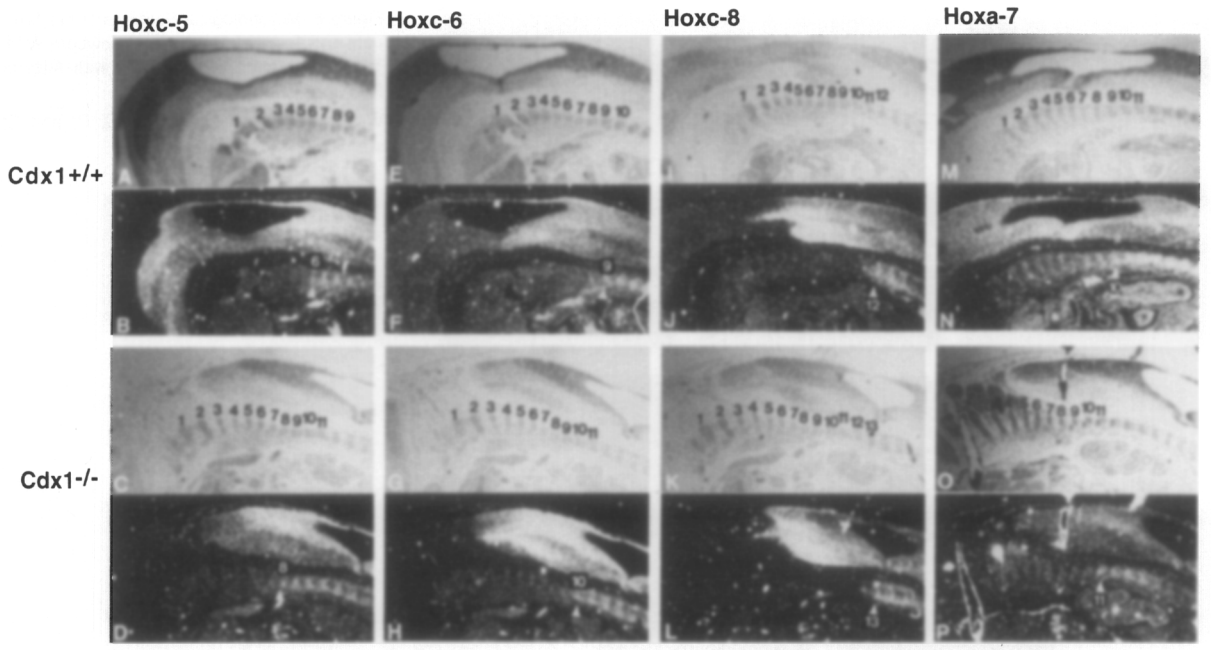

Figure 8. *Hox* Gene Expression in *Cdx1*$^{-/-}$ and Wild-Type 12.5 dpc Mouse Embryos

(A), (E), (I), and (M) are bright-field photomicrographs, and (B), (F), (J), and (N) are dark-field photomicrographs, respectively, of the wild type. (C), (G), (K), and (O) are bright-field photomicrographs, and (D), (H), (L), and (P) are dark-field photomicrographs of mutant mice.
The prevertebrae are numbered in the bright-field photographs, and the anterior boundaries of strong expression are indicated by number and arrow in the dark-field photographs.

analyses allow the prediction of a *caudal*-type DNA-binding motif.

We discovered the presence of this binding site (TTTATG) in the available regulatory sequences of 18 *Hox* genes in mouse and human. In most of these *Hox* genes, one or two putative *Cdx1*-binding sites are positioned directly 5′ of the transcription start site. In addition, up to four TTTATG motifs are located within the first intron (average size, 500 bp) (Figure 10A). Of special interest is the finding of two *Cdx1* putative binding sites within a 470 bp 5′ region of the *Hoxa-7* promoter (Figure 10B). Transgenic analyses have previously shown that this promoter region is sufficient to specify the anterior boundary of *Hoxa-7* (Knittel et al., 1995).

In an attempt to characterize the *Cdx1* function on *Hox* genes further, we performed *Cdx1* transactivation experiments on different *Hoxa-7 lacZ* promoter constructs in P19 cells. All *Hoxa-7 lacZ* constructs show basal level activity if transfected with a cytomegalovirus (CMV) control plasmid (Matthias et al., 1989). Cotransfection of a CMV–*Cdx1* expression plasmid with the AX 470 construct leads on average to a 3-fold induction. The construct carrying this promoter fragment in the reverse orientation (AX 470 reverse) cannot be induced. Deletion of a region including one putative *Cdx1*-binding site (construct AX 110–470) reduces the activation by 50% (Figure 10B). These results demonstrate the transactivation of *Hoxa-7* by *Cdx1* in tissue culture, suggesting regulatory interaction of *Cdx1* with the *Hoxa-7* promoter, most likely through the TTTATG sequence motif.

Discussion

Phenotype of *Cdx1*$^{-/-}$ Mice

We have generated homozygous mutant mice for the murine homeobox gene *Cdx1* that are viable and fertile. The phenotypic consequences of this mutation are anterior homeotic transformations of vertebrae.

In the *Cdx1* mutant mice, the mesodermal cells, which normally develop into the first vertebra, have undergone an anterior transformation, leading to aberrations of the basioccipital bone. From the first vertebra up to the seventh, the anterior transformations are quite clear, although, in many of the mutants, only unilateral. On the basis of the number and articulation of the ribs, we identified additional anterior homeotic transformations down the axis up to the midthoracic region, while no morphological changes are apparent posterior to T9.

Homeotic transformations have been described for mouse mutants generated by gene disruption for several of the *Hox* genes. In the *Hoxa-5* mutants, there is a posterior transformation of cervical vertebra 7 into the first thoracic vertebra (T1) with a pair of ribs (Jeannotte et al., 1993); *Hoxb-4* disruption leads to the partial homeotic transformation of the atlas to the axis and defects in the closure of the sternum (Ramírez-Solis et al., 1993). Mice that are mutant for *Hoxc-8* show anterior vertebral transformation and the generation of an extra pair of ribs from the first lumbar vertebra (Le Mouellic et al., 1992). The disruption of *Hoxd-3* (Condie and Capecchi, 1993) causes anterior transformations of the first and second cervical

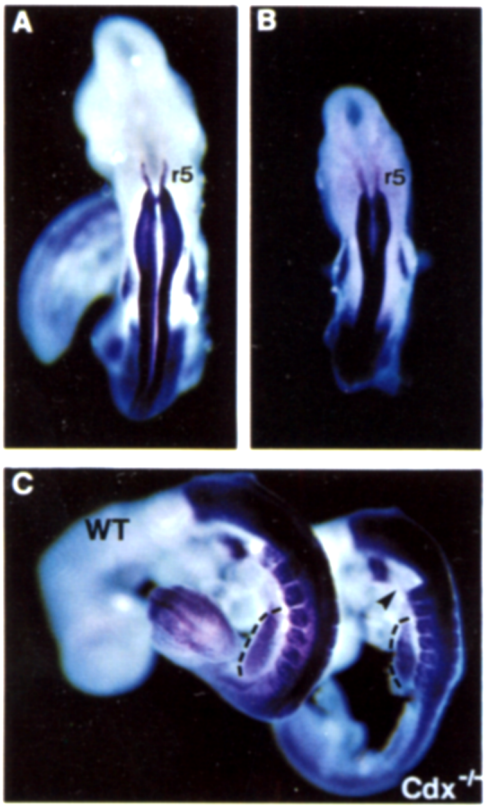

Figure 9. Whole-Mount In Situ Hybridization of *Hoxd-3* on *Cdx1* Mutant and Wild-Type Mice

(A) Dorsal view on a 9.5 dpc wild-type embryo; the rhombomere 5 is indicated as r5.
(B) Dorsal view of a 9.5 dpc *Cdx1*$^{-/-}$ embryo.
(C) Lateral view of a wild-type (left) and *Cdx1*$^{-/-}$ (right) embryo. The forelimb buds are marked by a dotted line. Arrow indicates the fifth somite in the mutant embryo, which lacks expression of *Hoxd-3*.

vertebrae, while the compound mutant *Hoxd-3/Hoxa-3* additionally shows the complete loss of an atlas vertebra (Condie and Capecchi, 1994). These results lead to the suggestion that there is more than one *Hox* gene coding for one segment and are in agreement with the *Hox* code (Kessel and Gruss, 1991). All these *Hox* gene disruptions have resulted in specific regional defects or transformation. In contrast, the *Cdx1* gene disruption causes a series of anterior transformations along the rostrocaudal axis.

Phenotypic alteration of axial skeletal structures also

Table 2. *Hox* Gene Expression in Wild-Type and *Cdx1* Mutant Mice

	Anterior Boundary of Expression in	
Hox Gene	*Cdx1*$^{+/+}$	*Cdx1*$^{-/-}$
Hoxa-7	pv 10	pv 11
Hoxc-5	pv 6 weak, pv 7 strong	pv 7 weak, pv 8 strong
Hoxc-6	pv 8 weak, pv 9 strong	pv 9 weak, pv 10 strong
Hoxc-8	pv11 weak, pv12 strong	pv 12 weak, pv 13 strong
Hoxd-3	somite 5	somite 6

Abbreviation: pv, prevertebra.

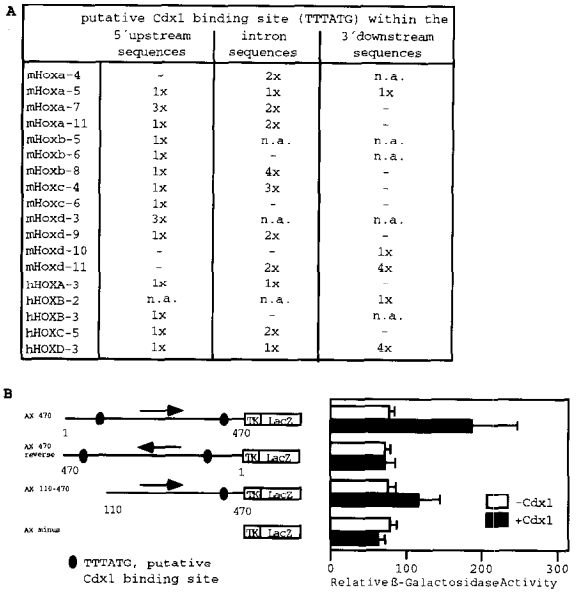

Figure 10. Potential *Cdx1*-Binding Sites in *Hox* Regulatory Regions and Transactivation In Vitro

(A) Putative *Cdx1*-binding motif, TTTATG, within regulatory sequences of murine and human *Hox* genes. Available sequences (EMBL databank) of 18 *Hox* genes have been searched for the TTTATG motif. If sequences were not available, the figure has been marked as n.a.
(B) Transactivation of *Hoxa-7 lacZ* reporter constructs by cotransfection of CMV–*Cdx1* in P19 cells. The *Hoxa-7 lacZ* reporter constructs are shown, and the position of the potential *Cdx1*-binding sites are indicated. The relative values of β-galatosidase activity of four independent experiments are illustrated.

occurred in gain-of-function mutants generated for *Hoxa-7* and *Hoxd-4*. In the case of *Hoxa-7* overexpression, the atlas and the axis acquired the characteristics of more posterior vertebrae and an additional vertebra: the proatlas was present (Kessel et al., 1990). Ectopic expression of *Hoxd-4* resulted in the absence or reduction in the supraoccipital and exoccipital bones of the skull and the presence of additional neural arches. Also, agenesis of the basisphenoid and the fusion of the atlas and axis with the basioccipital bone has been observed (Lufkin et al., 1992).

Similar malformations of the skull and the cervical vertebral column were reported after RA treatment of 7.4 dpc embryos (Kessel and Gruss, 1991). In the RA-treated embryos, the axial abnormalities included the appearance of a proatlas in 58% of the animals studied, as well as a rib anlage on vertebra 7 and one or two tuberculi anterior on vertebra 5 instead of vertebra 6. In addition, these mice exhibit dramatic aberrations of the skull, including a strong reduction of the supraoccipital, exoccipital, and basioccipital bones and structures anterior to these. In these mice, the boundaries of expression of at least three *Hox* genes were found to be shifted anteriorly, explaining the posterior transformations along the axis. In general, it was concluded that the loss or reduction of the *Hox* gene domains cause anterior transformations, while the extension of these domains causes posterior transformations.

The *Cdx1*$^{-/-}$ mice exhibit an incomplete first vertebrae,

which is fused to the basioccipital bone. On superficial examination, it resembles the proatlas phenotype seen in the gain-of-function experiments with *Hox* genes. However, the dramatic loss of structures of the skull, in particular the strong reduction of the basioccipital, exoccipital, and supraoccipital bones seen in *Hox* overexpression or RA treatment experiments, do not occur. On the contrary, the basioccipital bone in the *Cdx1*$^{-/-}$ mice appears strongly enlarged, arguing for an anteriorization of the mesodermal material that normally should form the first vertebra, while the so-called proatlas material has developed normally. This interpretation of the morphology of the *Cdx1*$^{-/-}$ mice is strongly supported by the posterior shifts of *Hoxd-3* expression from somite 5 to somite 6. Because of this shift, the expression domains of more anteriorly expressed *Hox* genes become extended, leading to an anteriorization of somite 5, which results in an extension of the basioccipital bone at later stages of development.

The series of homeotic transformations that we see in the *Cdx1* mutant mice correlate with an effect on several *Hox* genes. In situ hybridization analyses of *Hox* genes in the *Cdx1*$^{-/-}$ mice demonstrated a posterior shift of their expression domains in the somitic mesoderm by one segment.

Recently it has been reported that a targeted deletion of the *bmi-1* proto-oncogene (van Lohuizen et al., 1991a, 1991b), which shares several conserved domains with the *posterior sex combs reduced* gene from Drosophila (Jürgens, 1985), leads to posterior homeotic transformations along the rostrocaudal axis (van der Lugt et al., 1994). In contrast, the *Cdx1* mutation causes anterior rather than posterior homeotic transformations of vertebrae. On the basis of data from Drosophila, members of the *Polycomb* family are believed to form protein complexes that facilitate or regulate the formation of condensed chromatin, thereby repressing homeotic genes (for review see Paro, 1990). In contrast, the *caudal*-type homeobox genes are believed to function as activating transcription factors. For example, the Drosophila homolog *caudal* activates the segmentation gene *ftz* by direct binding of the sequence motif TTTATG (Dearolf et al., 1989). The presence of several putative *caudal*-type binding sites within the regulatory sequences of *Hox* genes and our in vitro transactivation experiments of *Cdx1* on *Hoxa-7* argue also for a direct activating function of *Cdx1* on *Hox* genes. Therefore, the physical basis for the function of *bmi-1* and *Cdx1* would appear to be different. In addition, the *bmi-1* gene seems to function only on members of the *Hoxc* cluster (van der Lugt, 1994), while we demonstrate the effect of *Cdx1* on *Hox* genes from three different clusters.

In the mouse, two other genes of the *Cdx* family, *Cdx2* and *Cdx4*, have been identified. Both genes are active early in gastrulation (Gamer and Wright, 1993; V. S., unpublished data) and show a partial overlapping expression pattern with *Cdx1* in the posterior part of the embryo. Therefore, the restricted phenotype of the *Cdx1* mutation to the anterior axis can be explained by complementary functions. In addition, *Cdx1* (V. S., unpublished data) and *Cdx2* (James and Kazenwadel, 1991) are expressed in overlapping patterns in the developing and adult intestine, indicating the different roles of *Cdx* genes. The possible effect of *Cdx1* disruption in the developing intestine is currently being investigated.

Molecular Mechanisms Mediating Homeotic Transformations in *Cdx1*$^{-/-}$ Mice: Effect on the *Hox* Code

How does the early expression pattern of the *Cdx1* gene correlate with the phenotype of the mutant mice? *Cdx1* is expressed at gastrulation, when the polarity and regionalization of the embryo is set up.

The formation of the primitive streak leads to the orderly ingression of cells from the epiblast to form the mesoderm and the endoderm (Bellairs, 1986). The paraxial mesodermal cells pass anteriorly, and from here, groups of cells are segmented off as somites (Flint, 1977; Tam and Beddington, 1986), which differentiate into the dermamyotome and the sclerotome cell lineages. Transplantation experiments in the chick showed that cells have knowledge about their future axial identity even before the formation of somites is apparent (Kieny et al., 1972). The initiation of somite formation at the anterior end of the embryo and region-specific time of their formation require positional information.

The large group of clustered *Hox* genes shows an orderly, temporal appearance along the primitive streak, beginning around 7.25 dpc, indicating their involvement in axial patterning (for review see Hunt and Krumlauf, 1992).

Cdx1 is first expressed at 7.5 dpc along the entire primitive streak (Meyer and Gruss, 1993). The onset of expression of the third paralogous *Hox* group is coincident with that of *Cdx1*. When the anterior boundaries of the third paralogous *Hox* gene are established, the expression of *Cdx1* declines (Meyer and Gruss, 1993), becomes more posterior, and is finally no longer detectable along the axis once specification is set up via the *Hox* genes.

The temporal coincidence in expression of members of the third paralogous group with *Cdx1* correlates very well with the similarity in phenotypic alterations seen in the *Cdx1* and *Hoxd-3*/*Hoxa-3* mutants (Condie and Capecchi, 1993). *Hoxd-3*$^{-/-}$ mice show a similar broadening of the basioccipital bone and fusion of the first vertebra to it (Condie and Capecchi, 1993). On the basis of our in situ data and the skeletal phenotype, we know that the *Hox* gene products have not been abolished. However, we see a clear shift in the domains of their expression in the somites. The restricted alteration of *Hox* expression domains in the mesoderm in the *Cdx1* mutant mice makes it very unlikely that *Cdx1* is involved in the initial activation of *Hox* genes within the primitive streak; otherwise, the ectodermal lineage should also be affected. However, a continued presence of *Cdx1* seems to be necessary for the correct axial specification of the somites. In the vertebrates, the specification of embryonic levels through the clustered homeobox genes seems to take place before segmentation occurs. Therefore, further regulatory controls may be needed to ensure that the correct *Hox* genes are expressed in the newly formed somites, to specify their identity. We would like to argue from our mutation and transactivation studies

that *Cdx1* functions in this process to set up the correct expression domains of *Hox* genes in the newly formed somites via direct *Hox* gene regulation.

Comparison of the Murine *Cdx1*$^{-/-}$ Phenotype with the Mutant and Ectopic Expression Phenotype of the Drosophila *caudal* Gene

The overall picture of the expression patterns of the *Cdx1* gene and the Drosophila *caudal* gene appear similar. Both these genes are expressed in a gradient with highest expression in the posterior part of the embryo (Macdonald and Struhl, 1986; Meyer and Gruss, 1993). From the two main studies with the *caudal* gene in Drosophila, the following salient features of the function of this gene emerge. McDonald and Struhl found that there was an alteration in segmentation, and the expression of the pair rule gene *ftz* was affected over a large region in *caudal* mutants. It is likely that the protein encoded by *caudal* regulates the expression of pair rule and homeotic genes either directly or via its effects on specific gap genes. Ectopic expression of *caudal* in the anterior end of the cellular blastoderm was found to disrupt head development and segmentation, owing to the altered expression of *ftz* and *engrailed*, as well as the repression of head-determining genes such as *deformed* (Mlodzik et al., 1990). DNA binding studies showed that *caudal* directly activates *ftz* (Dearolf et al., 1989). These results demonstrate the regulatory interaction of the *caudal* gene with the genes of the *Ant–Bx* complex. In the mouse, too, it is likely that the *Cdx1* gene has similar interactions.

In conclusion, we propose that the *Cdx1* gene plays a key regulatory role in the generation of the anteroposterior axial skeletal identity in mammals. The molecular mechanism may be due to direct effects on the *Hox* genes.

Experimental Procedures

Construction of Targeting Vectors

A 4.1 kb HindIII genomic fragment of *Cdx1*, obtained from a C57/BL6 genomic library, was used to generate the targeting construct. The *neo* gene was cloned into the unique BglII site within the third exon of *Cdx1* in the opposite transcriptional orientation. The herpes simple virus thymidine kinase (*HSV tk*) was inserted 3′ of the genomic sequences as the negative selection marker.

Generation of *Cdx1* Mutant Mice

The ES cell line R1 (Nagy et al., 1990) was cultured on mitomycin C–treated primary mouse fibroblasts with 100 U/ml of LIF, according to standard protocols (Mansour et al., 1988). ES cells were electroporated with 25 μg of linearized targeted vector and selected by use of 250 μg/ml G418 and 2 mM gancyclovir. The initial screening of positive ES cell clones was done by polymerase chain reaction (PCR). For this, the following primers were used: *neo* 5′ (5′-atgagagcagccgattgtctgttgtgccc) and *Cdx* 3′ (5′-agctggcacagagtctctgggtagagaaag). The PCR conditions were as follows: 94°C for 3 min, 55°C for 2 min, 72°C for 5 min, 94°C for 1 min, 55°C for 2 min, and 72°C for 1 min for 40 cycles. Southern blot analysis to verify the PCR products was performed by using a XbaI–HindIII fragment and a SmaI fragment 3′ of the targeting construct.

For the identification of *Cdx1*$^{+/+}$, *Cdx1*$^{-/+}$, and *Cdx1*$^{-/-}$ mice, we used the following PCR primers: 5′-ggctccttggcccggcgg and 5′-ccgagctggctgctaacc. The PCR conditions were as follows: 94°C for 3 min, 35 cycles of 68°C for 1.5 min, 94°C for 1 min, 68°C for 1.5 min, and 72°C for 10 min for 35 cycles.

Chimeras were generated either by aggregation of four to six targeted ES cells to NMRI morulae (Joyner, 1993) or by injection of six to eight cells into C57BL6 blastocysts (Hogan et al., 1986).

Generation of *Cdx1*$^{-/-}$ × L17 Mice and X-Gal Staining of Embryos

Homozygous *Cdx1* mutant mice were crossed with heterozygous mice of the L17 transgenic line (Püschel et al., 1990) to generate *Cdx1*$^{-/-}$/L17$^{+/-}$ embryos. Whole embryo X-gal staining was performed as described previously (Püschel et al., 1991).

In Situ Hybridization

In situ hybridization on sections of 12.5 dpc embryos was performed as described previously (Kessel and Gruss, 1991). For whole-mount in situ hybridization, 9.0–9.5 dpc mouse embryos were fixed and processed as previously described (Wilkinson, 1992). [^{35}S]RNA probes were generated according to standard protocols.

The probes used for in situ hybridization were the following: *Hoxa-7* (Püschel et al., 1990), *Hoxc-8* (Breier et al., 1986), and *Hoxc-6* and *Hoxc-5* (Sharpe et al., 1988). The *Hoxd-3* probe was a gift of M. R. Capecchi (Condie and Capecchi, 1993).

Skeletal Preparations

Skeletal preparations were made from 3-week-old adult mice as well as newborn mice, as described by Kessel et al. (1990).

Western Blotting

Protein extracts were prepared from intestines from *Cdx1*$^{-/-}$ and *Cdx1*$^{+/+}$ mice, and Western blot analysis was performed as described by Meyer and Gruss (1993).

Transactivation in Tissue Culture

The *Cdx1* cDNA was inserted into the expression vector pEVRF2 (Matthias et al., 1989) to drive expression under the control of the human CMV promoter enhancer. The *Hoxa-7 lacZ* reporter plasmids have been described by Knittel et al. (1995). P19 cells were grown in DMEM (Biochrom) supplemented with 10% fetal calf serum (Boehringer Mannheim) and transfected on 50 mm tissue culture dishes by the calcium phosphate method. We cotransfected 2.5 μg of the effector plasmid (CMV–*Cdx1* or the pEVRF2 vector without insert) and 2.5 μg of the reporter plasmids (AX 470; AX 470 reverse; AX110–350 or AX minus). Cells were harvested about 48 hr after transfection, and β-galactosidase activity assays were performed as described by Miller (1972).

Acknowledgments

We are especially grateful to Ahmed Mansouri for his help in generating the targeted ES cells. We would like to thank Michael Kessel, Peter Thorogood, Mike Akam, Robert Presley, and members of the Gruss lab for critical comments and valuable discussions. We would also like to thank Ralph Altschäffel for assistance with the illustrations, and the staff of the animal house, Max Planck Institute, Göttingen, and Lesley Moore, Bath University, for help in the generation and care of the mutants. V. S. would like to thank Ravi Acharya, Tony Rees, Kathryn Robson, and Kamal Chowdhury for their encouragement. During a part of this investigation, V. S. was supported by the Max Planck Society and the British Council. B. M. was supported by the Hochschule Sonderprogramm II. Most of the work was supported by the Max Planck Society and the Deutsche Forschungsgemeinschaft. Additional support was provided by the Human Frontiers Science Program. V. S. also thanks the Medical Research Council, United Kingdom, for support.

Received May 1, 1995; revised September 26, 1995.

References

Bellairs, R. (1986). The primitive streak. Anat. Embryol. *174*, 1–14.

Blumberg, B., Wright, V.E., De Robertis, E.M., and Cho, K.W.Y. (1991). Organizer-specific homeobox genes in *Xenopus laevis* embryos. Science *253*, 194–196.

Breier, G., Bucan, M., Francke, U., Colberg-Poley, A.-M., and Gruss, P. (1986). Sequential expression of murine homeobox genes during F9 EC cell differentiation. EMBO J. *5*, 2209–2215.

Bürglin, T.R., Finney, M., Coulson, A., and Ruvkun, G. (1989). *Caenorhabditis elegans* has scores of homoeobox-containing genes. Nature *341*, 239–243.

Capecchi, M.R., Capecchi, N.E., Hughes, S.H., and Wahl, G.M. (1974). Selective degradation of abnormal proteins in mammalian tissue culture cells. Proc. Natl. Acad. Sci. USA *71*, 4732–4736.

Condie, B.G., and Capecchi, M.R. (1993). Mice homozygous for a targeted disruption of *Hoxd-3* (*Hox-4.1*) exhibit anterior transformations of the first and second cervical vertebrae, the atlas and the axis. Development *119*, 579–595.

Condie, B.G., and Capecchi, M.R. (1994). Mice with targeted disruptions in the paralogous genes *hoxa-3* and *hoxd-3* reveal synergistic interactions. Nature *370*, 304–307.

Dawes, B. (1930). The development of the vertebral column in mammals, as illustrated by its development in *Mus musculus*. Phil. Trans. Roy. Soc. (Lond.) B *218*, 155–170.

Dearolf, C.R., Topol, J., and Parker, C.S. (1989). The *caudal* gene product is a direct activator of *fushi tarazu* transcription during *Drosophila* embryogenesis. Nature *341*, 340–343.

Duprey, P., Chowdhury, K., Dressler, G., Balling, R., Simon, L. D., Guénet, J.-L., and Gruss, P. (1988). A mouse gene homologous to the *Drosophila* gene *caudal* is expressed in epithelial cells from the embryonic intestine. Genes Dev. *2*, 1647–1654.

Flint, O.P. (1977). Cell Interactions in the Developing Axial Skeleton in Normal and Mutant Mouse Embryos (Cambridge: Cambridge University Press).

Frumkin, A., Rangini, Z., Ben-Yehuda, A., Gruenbaum, Y., and Fainsod, A. (1991). A chicken *caudal* homologue, *CHox-cad*, is expressed in the epiblast with posterior localization and in the early endodermal lineage. Development *112*, 207–219.

Gamer, L.W., and Wright, C.V.E. (1993). Murine *Cdx-4* bears striking similarities to the *Drosophila caudal* gene in its homeodomain sequence and early expression pattern. Mech. Dev. *43*, 71–81.

German, M.S., Wang, J., Chadwick, R.B., and Rutter, W.J. (1992). Synergistic activation of the insulin gene by a LIM-homeo domain protein and a basic helix-loop-helix protein: building a functional insulin minienhancer complex. Genes Dev. *6*, 2165–2176.

Hogan, B.L.M., Constantini, F., and Lacy, E. (1986). Manipulating the Mouse Embryo: A Laboratory Manual (Cold Spring Harbor, New York: Cold Spring Harbor Laboratory Press).

Hunt, P., and Krumlauf, R. (1992). *Hox* codes and positional specification in vertebrate embryonic axes. Annu. Rev. Cell. Biol. *8*, 227–256.

James, R., and Kazenwadel, J. (1991). Homeobox gene expression in the intestinal epithelium of adult mice. J. Biol. Chem. *266*, 3246–3251.

Jeannotte, L., Lemieux, M., Charron, J., Poirier, F., and Robertson, E.J. (1993). Specification of axial identity in the mouse: role of the *Hoxa-5* (*Hox1.3*) gene. Genes Dev. *7*, 2085–2096.

Joly, J.S., Maury, M., Joly, C., Duprey, P., Boulekbache, H., and Condamine, H. (1992). Expression of a zebrafish *caudal* homeobox gene suggests its involvement in the establishment of posterior cell lineage at gastrulation. Differentiation *50*, 75–87.

Joyner, A.L. (1993). Gene Targeting: A Practical Approach (Oxford: IRL Press).

Jürgens, G. (1985). A group of genes controlling the spatial expression of the bithorax complex in *Drosophila*. Nature *316*, 153–155.

Kenyon, C. (1986). A gene involved in the development of the posterior body region of C. elegans. Cell *46*, 477–487.

Kessel, M., and Gruss, P. (1991). Homeotic transformations of murine vertebrae and concomitant alteration of *Hox* codes induced by retinoic acid. Cell *67*, 89–104.

Kessel, M., Balling, R., and Gruss, P. (1990). Variations of cervical vertebrae after expression of a *Hox-1.1* transgene in mice. Cell *61*, 301–308.

Kieny, M., Mauger, A., and Sengel, P. (1972). Early regionalization of the somitic mesoderm as studied by the development of the axial skeleton of the chick embryo. Dev. Biol. *28*, 142–161.

Knittel, T., Kessel, M., Kim, M.H., and Gruss, P. (1995). A conserved enhancer of the human and murine *Hoxa-7* gene specifies the anterior boundaries of expression during embryonal development. Development *121*, 1077–1088.

Krumlauf, R. (1994). *Hox* genes in vertebrate development. Cell *78*, 191–201.

Le Mouellic, H., Lallemand, Y., and Brûlet, P. (1992). Homeosis in the mouse induced by a null mutation in the *Hox-3.1* gene. Cell *69*, 251–264.

Lufkin, T., Mark, M., Hart, C.P., Dollé, P., LeMeur, M., and Chambon, P. (1992). Homeotic transformation of the occipital bones of the skull by ectopic expression of a homeobox gene. Nature *359*, 835–841.

Macdonald, P.M., and Struhl, G. (1986). A molecular gradient in early *Drosophila* embryos and its role in specifying the body plan. Nature *324*, 537–545.

Mansour, S.L., Thomas, K.R., and Capecchi, M.R. (1988). Disruption of the proto-oncogene *int-2* in mouse embryo-derived stem cells: a general strategy for targeting mutations to non-selectable genes. Nature *336*, 348–352.

Margalit, Y., Yarus, S., Shapira, E., Gruenbaum, Y., and Fainsod, A. (1993). Isolation and characterization of target sequences of the chicken *CdxA* homeobox gene. Nucl. Acids Res. *21*, 4915–4922.

Matthias, P., Müller, M.M., Schreiber, E., Rusconi, S., and Schaffner, W. (1989). Eucaryotic expression vectors for the analysis of mutant proteins. Nucl. Acids Res. *17*, 6418.

Mavilio, F. (1993). Reulation of vertebrate homeobox-containing genes by morphogens. Eur. J. Biochem. *212*, 273–288.

McGinnis, W., and Krumlauf, R. (1992). Homeobox genes and axial patterning. Cell *68*, 283–302.

Meyer, B., and Gruss, P. (1993). Mouse *Cdx-1* expression during gastrulation. Development *117*, 191–203.

Miller, J.H. (1972). Experiments in Molecular Genetics (Cold Spring Harbor, New York: Cold Spring Harbor Laboratory Press).

Mlodzik, M., Fjose, A., and Gehring, W.J. (1985). Isolation of *caudal*, a Drosophila homeobox-containing gene with maternal expression whose transcripts form a gradient at the preblastoderm stage. EMBO J. *4*, 2961–2969.

Mlodzik, M., and Gehring, W.J. (1987). Expression of the *caudal* gene in the germ line of Drosophila: formation of an RNA and protein gradient during early embryogenesis. Cell *48*, 465–478.

Mlodzik, M., Gibson, G., and Gehring, W.J. (1990). Effects of ectopic expression of *caudal* during *Drosophila* development. Development *109*, 271–277.

Nagy, A., Gocza, E., Merentes Diaz, E., Prideaux, V.R., Ivanyi, E., Markkula, M., and Rossant, J. (1990). Embryonic stem cells alone are able to support fetal development in the mouse. Development *110*, 815–821.

Nagy, A., Rossant, J., Nagy, R., Abramow-Newerly, W., and Roder, J.C. (1993). Derivation of completely cell culture–derived mice from early passage embryonic stem cells. Proc. Natl. Acad. Sci. USA *90*, 8424–8428.

Northrop, J.L., and Kimelman, D. (1994). Dorsal–ventral differences in *Xcad-3* expression in response to FGF-mediated induction in *Xenopus*. Dev. Biol. *161*, 490–503.

Paro, R. (1990). Imprinting a determined state into the chromatin of *Drosophila*. Trends Genet. *6*, 416–421.

Püschel, A.W., Balling, R., and Gruss, P. (1990). Position-specific activity of the *Hox-1.1* promotor in transgenic mice. Development *108*, 435–442.

Püschel, A.W., Balling, R., and Gruss, P. (1991). Separate elements cause lineage restriction and specify boundaries of *Hox-1.1* expression. Development *112*, 279–287.

Ramírez-Solis, R., Zheng, H., Whiting, J., Krumlauf, R., and Bradley,

A. (1993). *Hoxb-4* (*Hox-2.6*) mutant mice show homeotic transformation of a cervical vertebra and defects in the closure of the sternal rudiments. Cell *73*, 279–294.

Rechsteiner, M. (1987). Ubiquitin mediated pathways for intracellular proteolysis. Annu. Rev. Cell Biol. *3*, 1–30.

Serrano, J., Scavo, L., Roth, J., De la Rosa, E.J., and De Pablo, F. (1993). A novel chicken homeobox-containing gene expressed in neurulating embryos. Biochem. Biophys. Res. Commun. *190*, 270–276.

Sharpe, P.T., Miller, J.R., Evans, E.P., Burtenshaw, M.D., and Gaunt, S.J. (1988). Isolation and expression of a new mouse homeobox gene. Development *102*, 397–407.

Suh, E., Chen, L., Taylor, J., and Traber, P.G. (1995). A homeodomain protein related to caudal regulates intestine-specific gene transcription. Mol. Cell. Biol. *14*, 7340–7351.

Tam, P.P.L., and Beddington, R.S.P. (1986). The metameric organization of the presomitic mesoderm and somite specification in the mouse embryo. In Somites in Developing Embryos, R. Bellairs, D.A. Ede, and J.W. Lash, eds. (New York: Plenum Press), pp. 17–36.

Tremblay, P., Kessel, M., and Gruss, P. (1995). A transgenic neuroanatomical marker identifies cranial neural crest deficiencies associated with the *Pax3* mutant *Splotch*. Dev. Biol., in press.

van der Lugt, N. (1994). Functional analysis of *Pim-1* and *Bmi-1* null-mutant mice. PhD thesis, University of Amsterdam, Amsterdam, The Netherlands.

van der Lugt, N.M.T., Domen, J., Linders, K., van Roon, M., Maandag, E.R., te Riele, H., van der Valk, M., Deschamps, J., Sofroniew, M., van Lohuizen, M., and Berns, A. (1994). Posterior transformation, neurological abnormalities, and severe haematopoietic defects in mice with targeted deletion of the *bmi-1* proto-oncogene. Genes Dev. *8*, 757–769.

van Lohuizen, M., Verbeek, S., Scheijen, B., Wientjens, E., van der Gulden, H., and Berns, A. (1991a). Identification of cooperating oncogenes in Eμ-myc transgenic mice by provirus tagging. Cell *65*, 737–752.

van Lohuizen, M., Frash, M., Wientjens, E., and Berns, A. (1991b). Sequence similarity between the mammalian *bmi-1* proto-oncogene and the *Drosophila* regulatory genes *Psc* and *Su(z)2*. Nature *353*, 353–355.

Waring, D.A., and Kenyon, C. (1990). Selective silencing of cell communication influences anteroposterior pattern formation in C. elegans. Cell *60*, 123–131.

Waring, D.A., and Kenyon, C. (1991). Regulation of cellular responsiveness to inductive signals in the developing *C. elegans* nervous system. Nature *350*, 712–715.

Wilkinson, D.G. (1992). In Situ Hybridization: A Practical Approach (London: Oxford University Press).

Xu, X., Xu, P., and Suzuki, Y. (1994). A maternal homeobox gene, *Bombyx caudal*, forms both mRNA and protein concentration gradients spanning anteriorposterior axis during gastrulation. Development *120*, 277–285.